Geochemical Journal, Vol. 36, pp. 255 to 269, 2002

Chemical process and environment of hydrothermal alteration of acidic volcanic rocks in the Mitsuishi district, southwest Japan

ATSUSHI NABETANI[1]* and NAOTATSU SHIKAZONO[2]

[1]Exploration Departments 1&2, INPEX Corporation, Shibuya-ku, Tokyo 150-0013, Japan
[2]Department of Applied Chemistry, Keio University, Kohoku-ku, Yokohama 223-8522, Japan

(*Received October 3, 2001; Accepted March 8, 2002*)

The Mitsuishi district, noted for the largest Roseki production in Japan, is generally characterized by the alteration zoning from center to margin; Quartz zone → Roseki ore (Pyrophyllite, Pyrophyllite-sericite and Sericite zones) → K-feldspar-sericite zone → Albite zone. They are overlain by Weakly propylitized zone. The filling temperatures of fluid inclusions in euhedral quartz crystals indicate the hydrothermal solution was about 300–350°C for the formation of Quartz zone. The chemical composition of the hydrothermal solution was estimated from salinity of the fluid inclusions, analytical results of altered rocks and minerals (feldspars and sericite), thermochemical calculations on the K-feldspar-albite and muscovite-paragonite solid solutions and equilibria in the Na_2O-K_2O-SiO_2-Al_2O_3-H_2O-HCl system, and mobility calculation on the water-rock interaction process. It is deduced that pH dramatically increased, while K and SiO_2 concentrations decreased, and Na concentration remained relatively constant in the hydrothermal solution from center to margin of the alteration zones.

INTRODUCTION

Rocks composed mainly of pyrophyllite, sericite and/or kaolinite with some amounts of other minerals such as quartz and pyrite are defined as "Roseki" in Japan.

The Mitsuishi district, southeastern part of Okayama Prefecture (Fig. 1), is well known as the area of the largest Roseki production in Japan. Therefore, this district has been studied by many workers mainly from geological points of view (e.g., Kimura, 1951; Kamitani and Fujii, 1972; Ishihara and Imaoka, 1999). It is generally accepted that the Roseki deposits in this district were formed with association of terrestrial volcanic activity of Cretaceous to Paleogene age (Shibata and Fujii, 1971; Kitagawa *et al*., 1988, 1999), and show a stratiform in shape occurring in hydrothermally altered acidic pyroclastic rocks (Fujii *et al*., 1971, 1979; Hirano *et al*., 1972).

In contrast to previous many studies, the Roseki deposits have not been mineralogically and geochemically studied well. Thus, in this paper, it is mainly intended to describe mineral assemblages, chemical compositions of bulk rocks and representative minerals in each alteration zone, and fluid inclusion data in an attempt to present a model of the chemical process of hydrothermal alteration around the most productive Roseki deposits, Daiyama area in the district.

GEOLOGICAL BACKGROUND

Figure 2 shows the columnar section of the original rocks in the Mitsuishi district mainly based on the present work with the aid of previous geological works (Omori, 1965, 1966; Fujii *et al*., 1979; Mitsuno and Omori, 1984).

Acidic (rhyolitic or dacitic) pyroclastic rocks of Late Cretaceous to Paleogene age

*Corresponding author (e-mail: anabetani@inpex.co.jp)

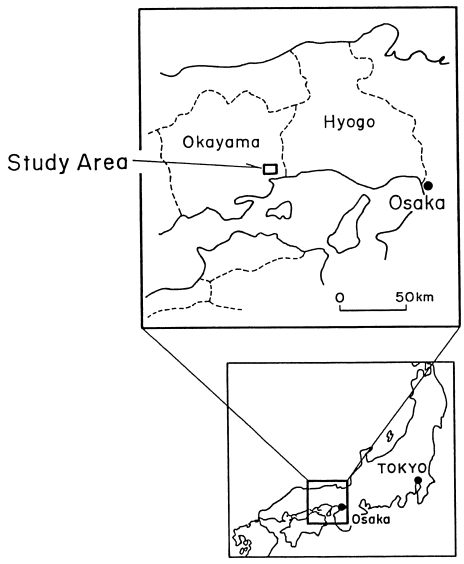

Fig. 1. Location map of the study area.

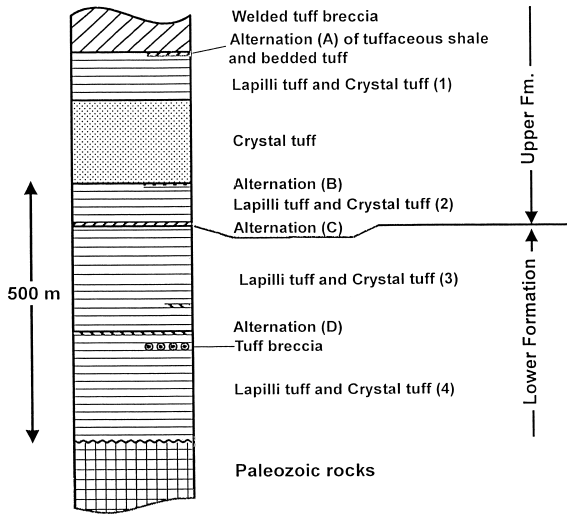

Fig. 2. Columnar section of the original rocks in the Mitsuishi district.

unconformably overlie the Paleozoic basement rocks exposed southeast of the Daiyama area. However, a part of the basement rocks is in fault contact with the acidic rocks. The acidic rocks generally strike N20°W to N30°E and dip 20° to 30°W. The acidic rocks are divided into the Upper and Lower Formations across Alternation (C) which consists of tuffaceous shale and bedded tuff.

The Lower Formation has undergone an intense hydrothermal alteration, especially in the horizon between Alternation (C) and (D), ranging in thickness from 200 to 300m. Quartz phenocrysts, shale fragments and eutaxitic texture are usually recognized as the original textures even in the rocks of Quartz zone which is mentioned in the next section.

In the Upper Formation, original textures are preserved well. Lapilli tuff is weakly welded. Crystal tuff is partly welded and contains a lot of subangular to angular phenocrysts of quartz and feldspars with diameter of 1 to 3 mm. Welded tuff breccia contains subangular to angular fragments, of acidic volcanic rocks and shales probably derived from the basement rocks, which are several mm to 4 cm in diameter.

Alteration Zoning and Mineral Assemblages

To clarify mineral assemblages of the altered acidic rocks collected not only from the Daiyama area but also from its vicinity, X-ray diffraction (XRD) analysis and observation of thin sections under an optical microscope were carried out for many samples. Distribution of alteration zones and mineral assemblages of each zone are obtained as shown in Figs. 3 and 4, respectively. Further study is necessary to present a three dimensional distribution of the alteration zones, and more regional zoning map.

Quartz zone

Quartz zone is distributed in four areas (A, B, C and D) as shown in Fig. 3. Quartz zone which seems to dip vertically is distributed in the areas A and B. Quartz zone in the area C is stratiform or vertically dips in part, lying between Alternation (C) and Roseki ore. The rocks of Quartz zone except in the area D are mostly porous.

The rocks of this zone are white to whitish gray in color, and composed mainly of quartz with some sericite and small amounts of pyrite, rutile, pyrophyllite and alunite. Porous quartz rocks hav-

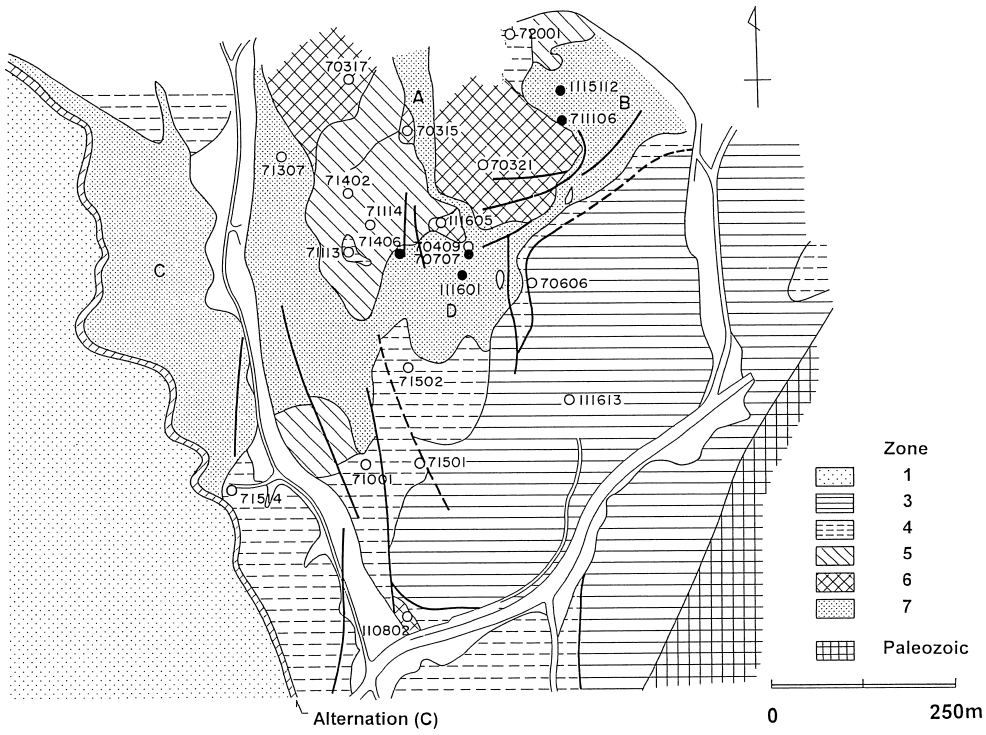

Fig. 3. Alteration zoning map in the Daiyama area. Open circle represents a site of the sample analyzed by XRF. Solid circle represents a site of the sample studied for fluid inclusions. 1. Weakly propylitized zone, 3. K-feldspar-sericite zone, 4. Sericite zone, 5. Pyrophyllite-sericite zone, 6. Pyrophyllite zone, 7. Quartz zone.

ing numerous pores of several mm in diameter are developed particularly near the boundary with Roseki ore. Some of their pores are filled with white sericite. Quartz rocks with white sericite filling most of pores are called “Fuiri-toseki” by local mining geologists. Pale green, chocolate or milky white vein-like shaped concretions composed of sericite with a few cm in width are also found near the boundary. The vari-colored concretions are referred to as “vein-like shaped sericite” hereinafter. Pyrophyllite seems to occur filling pores or fissures as sericite.

Roseki ore generally surrounds the Quartz zone in the horizon between Alternation (C) and (D). Most of Alternation (D) is also altered into the rocks of Roseki ore. Matrix and feldspar phenocrysts of the rocks are altered to clay minerals with quartz. Volcanic glass or pumice is altered to clay minerals. Black colored veins composed mainly of pyrite and quartz are often found in the ore. The veins are several ten cm in width and contain small amounts of white aggregates composed of smectite, sericite, kaolinite and/or pyrophyllite. Based on the predominant minerals besides quartz, the Roseki ore can be divided into the following three zones.

Pyrophyllite zone

Rocks of this zone are grayish white and composed mainly of pyrophyllite and quartz with small amounts of pyrite and rutile. Mixture of kaolinite and pyrophyllite called “Haku-roseki” by the local mining gelogists is sometimes recognized. Spherical or stick-like shaped concretions of diaspore often occur in the Haku-roseki. Both of the concretions are several to ten centimeters in diameter, and the stick-like ones are several ten centimeters in length.

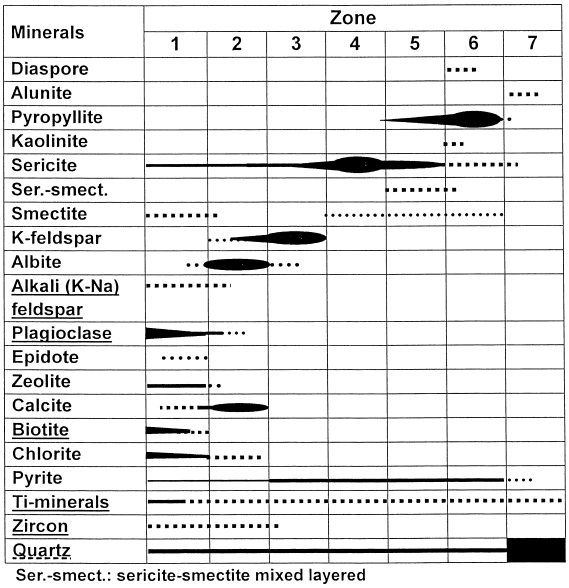

Fig. 4. Mineral assemblages in each alteration zone. 1. Weakly propylitized zone, 2. Albite zone, 3. K-feldspar-sericite zone, 4. Sericite zone, 5. Pyrophyllite-sericite zone, 6. Pyrophyllite zone, 7. Quartz zone. Primary in-situ minerals are underlined. The others are secondary altered minerals.

Pyrophyllite-sericite zone

Rocks of this zone are whitish gray and composed mainly of pyrophyllite, sericite and quartz with small amounts of pyrite and rutile. Most of the sericite are partly interstratified with smectite layers, having a broad peak of basal spacing (10.2–10.4Å). Smectite-sericite regularly mixed layered mineral having a basal spacing of 25Å is sometimes recognized.

Sericite zone

Rocks of this zone are pale greenish white, yellowish white or whitish gray and composed mainly of sericite and quartz with small amounts of pyrite and rutile. These rocks generally do not contain pyrophyllite, however, are referred to as "Roseki" by the local mining geologists.

K-feldspar-sericite zone

The Lower Formation is subjected to potassic alteration around the Roseki ore. Rocks of this zone are grayish white and composed mainly of K-feldpar, sericite and quartz with small amounts of pyrite and rutile. Feldspars and matrix are altered to K-feldspar with sericite and quartz. Volcanic glass or pumice is altered to greenish sericite. Pyrite nodules are often found. Aggregates of albite and K-feldspar conjectured to be precipitated at the later formation stage of this zone locally occur at small fault planes, where the amount of albite is larger than that of K-feldspar.

Albite zone

The Lower Formation has undergone extensive albitization around K-feldspar-sericite zone in the outside of the area shown in Fig. 3. Rocks of this zone are pale green to pale greenish gray, and are composed mainly of albite, quartz, sericite and calcite with small amounts of K-feldspar, alkali-feldpar, plagioclase, chlorite, pyrite and trace rutile and zircon. Although the original textures are mostly preserved, plagioclase is replaced by albite with calcite and sericite. Calcite is also disseminated in matrix apart from feldspars. Most of volcanic glass or pumice are altered to greenish sericite.

Weakly propylitized zone

The Upper Formation including Alternation (C) is generally weakly propylitized. The original textures and minerals are almost preserved. Rocks of this zone are composed mainly of plagioclase, quartz, chlorite and calcite, containing small amounts of alkali-feldspar, albite, sericite, biotite, pyrite, epidote, sphene and trace zircon. Matrix is dark greenish gray in color due to its weak chloritization. Amphibole is altered to chlorite, sometimes with epidote or sphene. Most of biotite is chloritized with sphene. Plagioclase is accompanied commonly by calcite or sometimes by sericite. Zeolite minerals (stilbite, Na-stilbite, laumontite), which are commonly recognized as joint-fills with narrow width, are conjectured to be precipitated after the major stage of the hydrothermal alteration.

Polytype of sericite

Two kinds of sericite polytype ($2M_1$ and 1M) are identified in a series of alteration zones. In Quartz zone the amount of $2M_1$ sericite is greater than or nearly equal to that of 1M for the white sericite in Fuiri-toseki, however, less than or nearly equal to that of 1M for the vein-like shaped sericite. In Roseki ore the amount of $2M_1$ sericite is not so different from that of 1M sericite. In other zones 1M sericite predominantly occurs.

It is generally accepted that $2M_1$ mica is more stable than 1M mica at higher temperatures (Yoder and Eugstar, 1955). Therefore, the occurrence of sericite polytypes seems to indicate the general decrease of temperature from Quartz zone toward outer zones during the hydrothermal alteration process.

Chemical Environment of Hydrothermal Alteration

Chemical compositions of altered rocks

Thirty eight altered rock samples collected from the Mitsuishi district were analyzed to obtain bulk rock chemical compositions by means of an automatic X-ray fluorescence spectrometer (XRF), Rigaku IKF 3064 adopting the glass disk method (Matsumoto and Urabe, 1980). Seventeen rocks of the thirty eight rocks were sampled from the Daiyama area (Fig. 3). Analytical results are given in Appendix and Fig. 5.

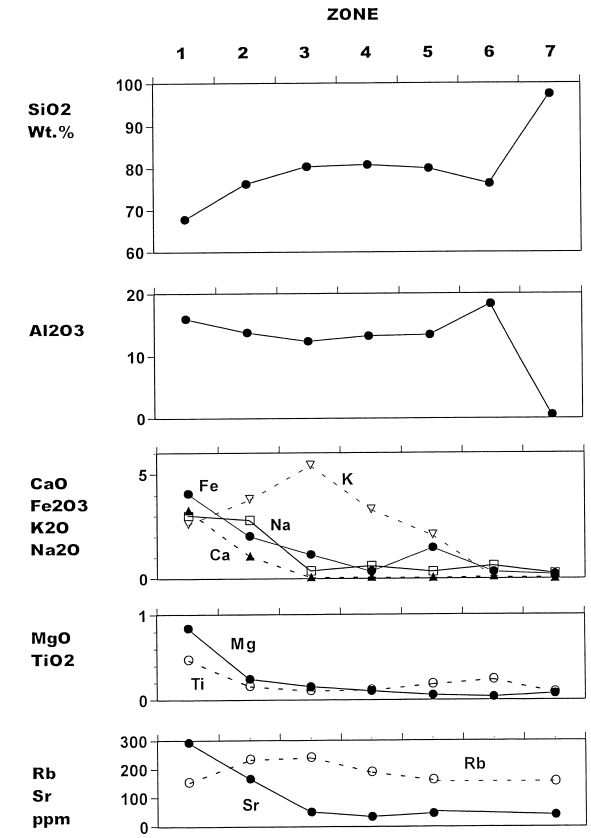

Fig. 5. Variations of the average chemical compositions of the rocks in each alteration zone. 1. Weakly propylitized zone, 2. Albite zone, 3. K-feldspar-sericite zone, 4. Sericite zone, 5. Pyrophyllite-sericite zone, 6. Pyrophyllite zone, 7. Quartz zone.

Temperature and salinity estimated by fluid inclusions

Euhedral quartz crystals often occur in the porous rocks of Quartz zone. The quartz crystals are 0.5 mm to 1 cm in length. Comparatively large crystals were examined under the microscope. They are highly transparent and contain many fluid inclusions with circulat, elliptical or rectangular shape. Most fluid inclusions are composed of vapor and liquid phases. The vapor phases are about 20–50% in volume percent.

Filling temperatures were measured for five quartz crystals which sampling sites are shown in Fig. 3. The temperatures for each sample generally range from 300° to 350°C without a wide scatter (Fig. 6). Salinities of the liquid phases estimated from the freezing temperatures for some of the inclusions range from 0.4 to 0.8 NaCl eq.wt.% (0.1 mol/l NaCl in average).

Activity ratio of Na^+ to K^+ of hydrothermal solution estimated from equilibria in the system Na_2O-K_2O-Al_2O_3-SiO_2-H_2O-HCl

We estimate the a_{Na^+}/a_{K^+} of hydrothermal solution for K-feldspar-sericite zone and the outer rim of Quartz zone based on the thermochemical consideration on the solid solutions in the system Na_2O-K_2O-Al_2O_3-SiO_2-H_2O-HCl.

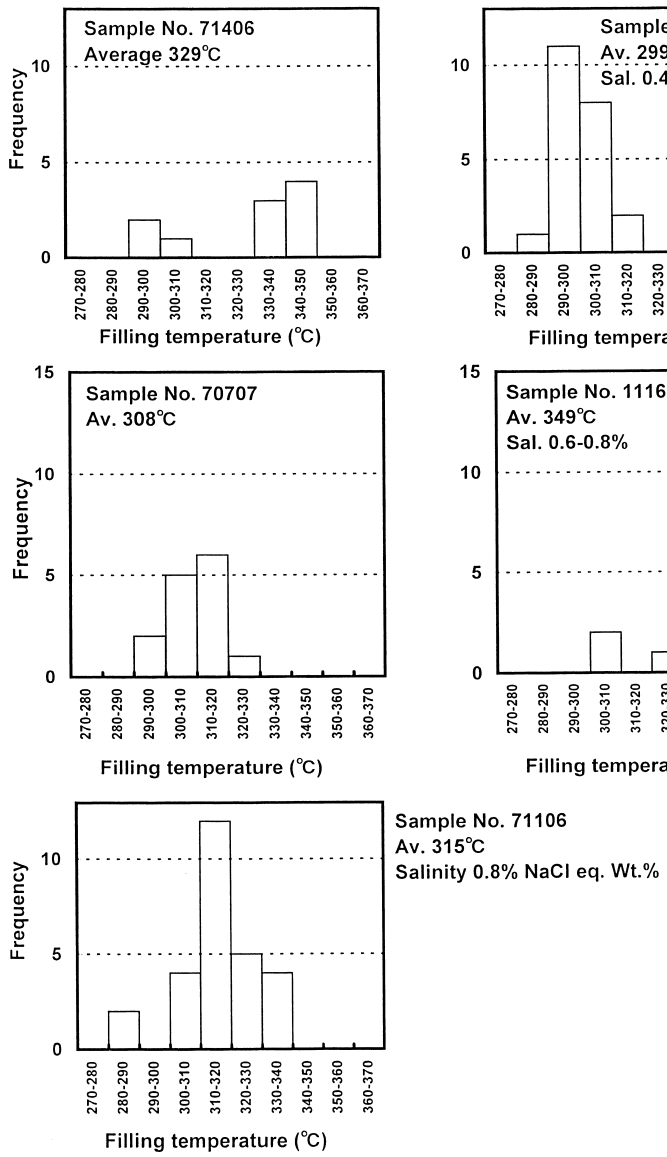

Fig. 6. Histograms of filling temperatures of fluid inclusions in the euhedral quartz crystals collected from Quartz zone.

Eugster *et al*. (1972) gave the excess free energy in cal/mol (G_{exl}) at T (K) and P bar from the solvus in the muscovite-paragonite system as follows:

$$G_{exl} = (3082.1 + 0.0822P + 0.1698T)X_{pag}X_{mus}^{2} + (4163.9 + 0.1259P + 0.3954T)X_{mus}X_{pag}^{2} \quad (1)$$

where X_{mus} and X_{pag} represent the mole fraction of muscovite and paragonite, respectively.

The white sericite in Fuiri-toseki which occurs in the outer rim of Quartz zone has the average compositions of X_{pag} = 0.037 (Table 1). Assuming that the temperature and pressure of hydrothermal solution were 350°C and 1 Kb, respectively, the a_{Na^+}/a_{K^+} of hydrothermal solution in

Table 1. Paragonite mole fractions (X_{pag}) in the sericite occurring in Quartz zone analyzed by atomic absorption method

Sericite occurrence	Sample No.	X_{pag}
Vein-like shaped	110813	0.068
	70322	0.100
	111015	0.059
(average)		(0.076)
in Fuiri-toseki	51512	0.054
	70707	0.030
	70415	0.032
	70307	0.033
(average)		(0.037)
Average	—	0.054

equilibrium with the sericite can be estimated to be 25.9 by using Eq. (1) and the thermochemical data in Table 2. The V° and Cp° coefficients for each ion species shown in Table 2, which are those at 250°C and 300°C, respectively, were used at any temperatures of the estimations.

The vein-like shaped sericite is richer in Na than the white sericite (Table 1), suggesting that the former sericite was precipitated at the higher activity ratio of Na^+ to K^+ than that of the latter one. The vein-like shaped sericite might be precipitated at the lower temperature alteration stage later than the formation of most of Quartz zone and Roseki ore.

Orville (1963) experimentally determined the solvus in the albite-K-feldspar binary system at 500°, 600°, 650°, 700°C and 2 Kb. Thompson and Waldbaum (1968) obtained the excess free energy in cal/mol (G_{ex2}) at T (K) and 2 Kb as follows, on the assumption that K·Na feldspar is the asymmetrical solid solution.

$$G_{ex2} = (-463 + 5.052T)X_{or}X_{ab}^2 + (5679 - 2.954T)X_{ab}X_{or}^2 \quad (2)$$

where X_{or} and X_{ab} represent the mole fraction of K-feldspar and albite, respectively.

In K-feldspar-sericite zone feldspars typically have the composition of X_{or} = 0.96–0.98 (average

Table 2. Thermochemical data for minerals, water and ion species at 298.15 K and 1 bar. Data for minerals and water are given by Helgeson et al. (1978); (d) by Robie and Waldbaum (1968); (e) by Helgeson (1969); (f) Partial molal volume (V°) at 250°C given by Ellis and McFadden (1972); (g) Cp° (isobaric heat capacity) coefficient at 300°C given by Helgeson (1969).

Minerals, etc.	ΔGf°	ΔHf°	ΔSf°	S°	V°	Cp° coefficients = a + bT + c/T²		
	(cal/mol)	(cal/mol)	(cal/mol·k)	(cal/mol·k)	(cm^3/mol)	a (cal/mol·k)	b (10^3 cal/mol·k^2)	c (10^{-5} cal/mol·k)
Pyropyllite	–1,255,997	–1,345,313	–299.6	57.2	126.6	79.432	39.214	–17.282
Low-albite	–886,308	–939,680	–179.0	49.51	100.07	61.70	13.90	–15.01
K-feldspar	–895,374	–949,188	–180.5	51.13	108.87	76.617	4.311	–29.945
Paragonite	–1,326,012	–1,416,963	–305.1	66.4	132.53	97.43	24.50	–26.44
Muscovite	–1,336,301	–1,427,408	–305.6	68.8	140.71	97.56	26.38	–25.44
Quartz	–204,646	–217,650	–43.6	9.88	22.688	11.22	8.20	–2.70
H_2O	–54,634	–57,796	–10.6	45.1	24,465	7.300	2.46	—
K^+	–67,700 (d)	–60,040 (e)	25.7	24.5 (e)	–19 (f)	43 (g)	—	—
Na^+	–62,589 (d)	–57,279 (e)	17.8	14.4 (e)	–29 (f)	49 (g)	—	—
H^+	0 (d)	0 (e)	0.0	0.0 (e)	–23 (f)	39 (g)	—	—

Table 3. Representative partial analysis data of feldspars obtained by EPMA. OR: K-feldspar; AB: albite; AN: anorthite.

K-feldspar-Sericite zone							
Point	1	2	3	4	5	6	7
Sample	70606	70606	110415	110415	110412	110402	110402
OR	96.94	97.10	95.76	96.22	97.42	96.87	96.60
AB	2.96	2.81	4.12	3.78	2.45	2.73	3.07
AN	0.10	0.09	0.12	0.08	0.13	0.40	0.33

0.97) as shown in Table 3. Assuming that the formation pressure was 1 Kb and G_{ex2} at 2 Kb = G_{ex2} at 1 Kb, the a_{Na^+}/a_{K^+} is estimated to be 3.5, 6.7, 15.4 and 44.4 at 350°, 300°, 250° and 200°C, respectively, by using Eq. (2) and the thermochemical data in Table 2.

DISCUSSION

Mobility of each component in the process of hydrothermal alteration

In view that the hydrothermal alteration was the weakest in intensity for Weakly propylitized zone among a series of alteration zones, the weakly propylitized rocks are assumed to be the original rocks in the following discussion.

Al_2O_3 must have been depleted from the original rocks during the formation of Quartz zone. However, most of the depleted Al_2O_3 would not be transported far from Quartz zone and fixed in the adjacent Pyrophyllite zone. On the other hand, in the alteration zones with the exception of Quartz zone and Pyrophyllite zone Al_2O_3 tended to behave like an inert component, since Al_2O_3 content is comparatively constant ranging from 11 to 16 wt.% except in Quartz and Pyrophyllite zones (Appendix, Fig. 5).

If a certain component has the same ratio to Al_2O_3 as that of the original rocks, it would be plotted on the line drawn on Fig. 7 for altered rocks. If a certain component plotted under the line, it is considered the component tended to be depleted from the original rocks to the hydrothermal solution. To the contrary, it is considered that the component plotted above the line had a tendency to be added from the solution.

These considerations lead to (1) SiO_2 tended to be added from the hydrothermal solution (Fig. 7A). However, SiO_2 plotted under the line for three samples from Pyrophyllite and Pyrophyllite-sericite zones might be due to the addition of Al_2O_3 to them; (2) CaO, MgO, Fe_2O_3 and TiO_2 tended to be depleted (Figs. 7B, C and F); (3) K_2O tended to be depleted in Quartz, Pyrophyllite and Pyrophyllite-sericite zones, however, to be added in Sericite, K-feldspar-sericite and Albite zones (Fig. 7D); (4) Neither large depletion nor large addition of Na_2O occurred in Albite zone. On the other hand, in K-feldspar-sericite zone, Roseki ore and Quartz zone Na_2O was depleted to the solution (Fig. 7E).

Mobility of each component is estimated more quantitatively on the basis of the following calculation. If the original rock (*A* (100 g)) was changed into the altered rock (*B*) by the addition of the component *i* (*Xi*) from hydrothermal solution and if *Ai* and *Bi* represent the wt.% of the component i in the rock (*A*) and that in the rock (*B*), respectively, on the assumptions that no H_2O is contained in the rocks (*A*) and (*B*) and that $X_{Al_2O_3}$ is zero, *Xi* values are calculated as shown in Fig. 8 from the following equation using the bulk rock average chemical compositions of each alteration zone (Appendix).

$$(Ai + Xi) \times 100/(100 + \sum Xi) = Bi. \qquad (3)$$

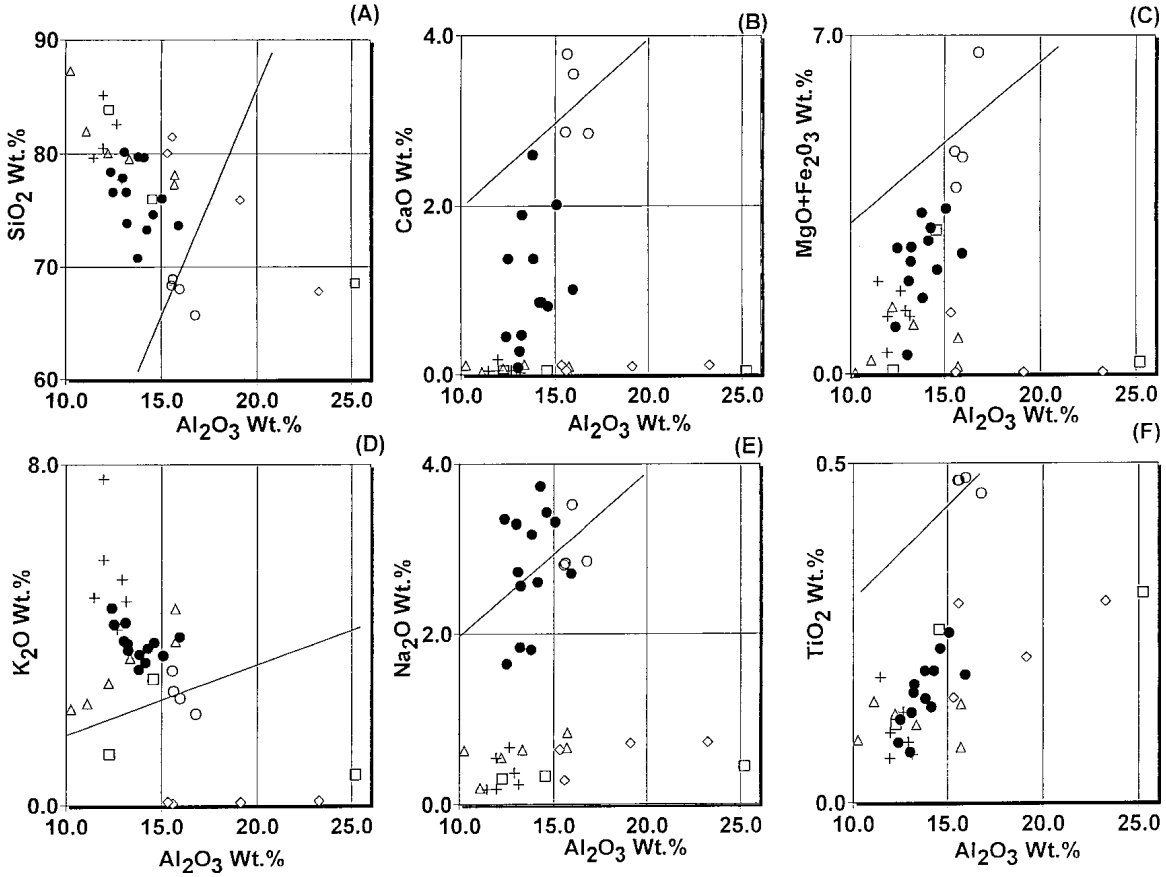

Fig. 7. Relationship between Al_2O_3 and other components. Rocks plotted on the line in each diagram have the same ratio to Al_2O_3 as that of the original rocks. (A) Al_2O_3-SiO_2, (B) Al_2O_3-CaO, (C) Al_2O_3-($MgO+Fe_2O_3$), (D) Al_2O_3-K_2O, (E) Al_2O_3-Na_2O, (F) Al_2O_3-TiO_2, ○: Weakly propylitized zone; ●: Albite zone; +: K-feldspar-sericite zone; △: Sericite zone; □: Pyrophyllite-sericite zone; ◇: Pyrophyllite zone.

Chemical process of hydrothermal alteration

Since the Upper Formation is not strongly altered, Alternation (C) might have acted as a cap rock for the infiltration of the hydrothermal solution. The formation of alteration zoning below Alternation (C) could be understood by the conceptual model, as illustrated in Fig. 9, which is under the assumptions that the infiltration of hydrothermal solution through the column of the original rocks was one-directional and that repetition of the infiltration did not occur.

Solution I is defined as the hydrothermal solution initially ascending through the column. Since Solution I could dissolve Al_2O_3 from the original rocks and precipitate much quartz, it is considered that Solution I was strongly acid and oversaturated with respect to SiO_2, and Fe, Ca, Mg, Al, Na, K and Ti were mostly dissolved from biotite, amphibole, alkali-feldspar, plagioclase and volcanic glass or pumice. As a result of the dissolution reactions, the concentration of these components in the solution increased, and the solution became less acid than Solution I.

Solution I would be about 300–350°C in temperature, which is estimated from the fluid inclusion study. The occurrence of sericite polytypes suggests that temperature of the solution tended to decrease as the solution infiltrated through the

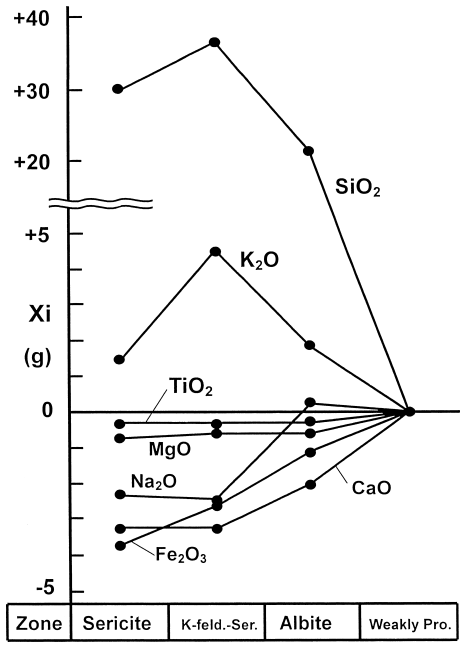

Fig. 8. Relative enrichment and depletion of components against Al_2O_3 in each zone.

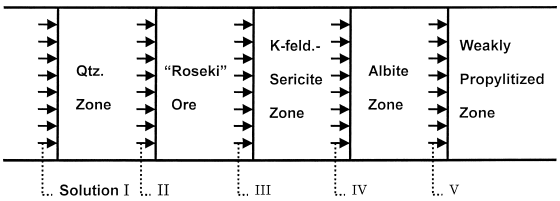

Fig. 9. Conceptual model of fluid flow during alteration process.

columm. The decrease in temperature resulted in the decrease in SiO_2 solubility, accompanying the continuous precipitation of quartz in the column.

Solution II, which is defined as the solution after the formation of Quartz zone, was able to alter the original rocks into Roseki ore. The original rocks were altered into K-feldspar-sericite zone by Solution III defined as the solution after the formation of Roseki ore, and into Albite zone by Solution IV defined as the solution after the formation of K-feldspar-sericite zone. These reactions caused a general increase in the concentrations of Mg, Ca, Fe and Ti in the hydrothermal solution. Solution V defined as the solution after the formation of Albite zone may become to be finally in equilibrium with the original rocks, although the weakly propylitized rocks which are assumed to be the original rocks in this discussion are limited to the Upper Formation in the study area.

By the above-process, potassium dissolved to the solutions during the formation processes of Quartz zone and most zones of Roseki ore would be partly fixed as sericite or K-feldspar in Sericite zone or K-feldspar-sericite zone, which caused a general increase in the ratio of Na to K in the solution. Aluminum dissolved from the original rocks during the formation of Quartz zone was mostly fixed as diaspore or pyrophyllite in the adjacent Pyrophyllite zone.

Chemical composition of hydrothermal solution responsible for the formation of Roseki ore and K-feldspar-sericite zone

We try to estimate the chemical composition of Solutions II and III from the stability relation between pure solid phases for the system Na_2O-K_2O-Al_2O_3-SiO_2-H_2O-HCl (Fig. 10) and thermochemical consideration mentioned in the previous section, assuming that the total pressure was 1 Kb and the activity of aqueous species, *a*, is equal to the molarity, *m*.

Since the mineral assemblage in Roseki ore is represented as pyrophyllite, sericite and quartz, if Solution II was 350°C in temperature, a_{K^+}/a_{H^+} of the solution is estimated to be $10^{2.10}$ from Fig. 10. As mentioned in the previous section, if Solution II was in equilibrium with K-Na mica solid solution having $X_{pag} = 0.037$ (Table 1), a_{Na^+}/a_{K^+} could be calculated to be 25.9 for the sericite in Fuiri-toseki at 350°C. Then, a_{Na^+}/a_{H^+} could be calculated to be $10^{3.51}$. The point indicating Solution II corresponds to be near the boundary between pyrophyllite and muscovite in Fig. 10.

Na^+ and K^+ are dominant species among cations at higher temperatures in usual geothermal waters (Ellis, 1970) as well as fluid inclusions (Roedder, 1979). If Solution II had the same salinity as fluid inclusions in Quartz zone being free

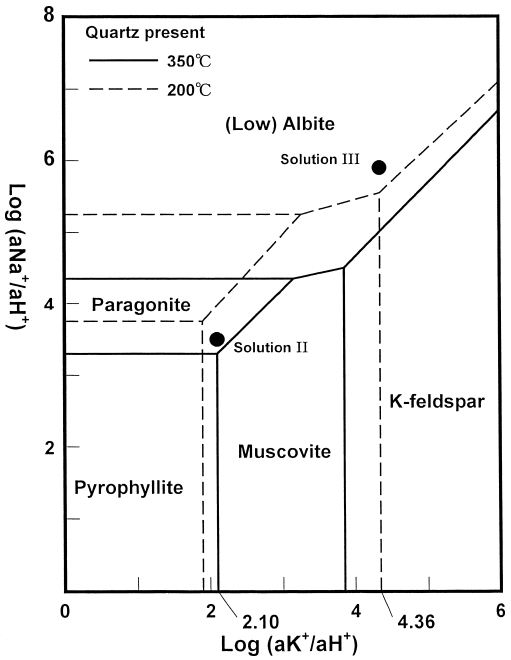

Fig. 10. Calculated mineral stability relation as a function of log (a_{Na^+}/a_{H^+}) vs. log (a_{K^+}/a_{H^+}) in the system Na_2O-K_2O-Al_2O_3-SiO_2-H_2O-HCl at 350°C and 200°C, 1 Kb, and quartz saturation. Thermochemical data used for the calculations are shown in Table 2.

from Ca, Mg, Fe and Ti: its $m_{Na^+} + m_{K^+}$ could be estimated as 0.10 from the salinity data. Consequently, it can be estimated that the solution responsible for the formation of Roseki ore had the composition of $m_{K^+} = 0.004$, $m_{Na^+} = 0.096$ and pH = 4.5.

In our conceptual model composition of Solution III was controlled only by the reaction between the original rocks and Solution II. If Roseki ore is represented by the rocks of Sericite zone in chemical compositions and if the original rocks (100 g) was altered into Sericite zone by Solution II (Y liters), it is considered on the basis of the mobility calculation (Fig. 8) that 2.34 g Na_2O (0.076 mol Na^+) was depleted from the original rocks and 1.41 g K_2O (0.030 mol K^+) was added from the solution to the rocks. Therefore, Solution III would have the composition of $m_{Na^+} = 0.096 + 0.076/Y$, and $m_{K^+} = 0.004–0.030/Y$. The a_{Na^+}/a_{K^+} ratio of the solution in K-feldspar-sericite zone has been already obtained in the previous section as 3.5, 6.7, 15.4 and 44.4 at 350°, 300°, 250° and 200°C, respectively.

Table 4. Chemical compositions of Solutions II and III. The temperature was assumed to be 350°C for Solution II and 200°C for Solution III.

Contents (ppm)	Solution II	Solution III
Na	2,210	2,320
K	160	100
Ca	—	170
Mg	—	30
Fe	—	190
Ti	—	10
SiO_2	1,320	320
pH	4.5	6.9

Y is calculated to be less than zero at 350°, 300° and 250°C, and to be greater than zero at 200°C. Since the solution volume must have been greater than zero, the temperature of Solution III was not higher than 250°C. In this discussion under the assumption that the temperature was 200°C, Y and m_{Na^+}/m_{K^+} are obtained to be 13.8 and 44.4, respectively. Therefore, m_{Na^+} and m_{K^+} are calculated to be 1.0×10^{-1} and 2.6×10^{-3}, respectively. The m_{K^+}/m_{H^+} of the solution in equilibrium with the assemblage of K-feldspar, sericite and quartz is estimated to be $10^{4.36}$ from Fig. 10. The pH is obtained to be 6.9 from the estimated m_{K^+}/m_{H^+} and m_{K^+}. Thus, a_{Na^+}/a_{H^+} is obtained to be $10^{5.9}$ which corresponds to be near the boundary between K-feldpar and muscovite in Fig. 10. The concentrations of other components can be estimated similarly as m_{K^+} and m_{Na^+}; $m_{CaT} = 0.058/Y$, $m_{MgT} = 0.018/Y$, $m_{FeT} = 0.023/Y$, $m_{TiT} = 0.004/Y$. Substituting Y into the above equations, we obtain $m_{CaT} = 4.2 \times 10^{-3}$, $m_{MgT} = 1.3 \times 10^{-3}$, $m_{FeT} = 1.7 \times 10^{-3}$, and $m_{TiT} = 3.1 \times 10^{-4}$, where "T" represents the total.

The estimated chemical compositions of Solutions II and III are summarized in Table 4, where the concentration of aqueous silica is estimated from the quartz solubility data by Hemley *et al.* (1980). The chemical compositions of Solutions

IV and V were not estimated because of many unknown factors such as the uncertainty of temperature estimate. The estimated chemical compositions indicate that m_{K^+} decreased slightly, m_{Na^+} was relatively constant, pH increased dramatically and SiO_2 concentration decreased from Solution II to Solution III.

If the volume (V) and average density (ρ) of the original rocks which were altered to Roseki ore are known, the total volume (Y_{total}) of Solution II can be estimated from the equation: $Y_{total} = Y(V\rho)/100$. V may be inferred from the total rock volume (V_{ore}) of Roseki ore. However, the density data are not available, and V_{ore} is unknown because of uncertainty of three dimensional distribution of the ore.

CONCLUSIONS

Important conclusions of this study are summarized as follows:

(1) The Mitsuishi district is characterized by the alteration zoning from center to margin; Quartz zone → Roseki ore (Pyrophyllite, Pyrophyllite-sericite and Sericite zones) → K-feldspar-sericite zone → Albite zone. They are overlain by Weakly propylitized zone.

(2) XRF analysis of the altered rocks indicates that (i) SiO_2 was added in most of alteration zones; (ii) Al_2O_3 tended to behave like an inert component in the alteration zones except Quartz and Pyrophyllite zones; (iii) CaO, MgO, Fe_2O_3 and TiO_2 were depleted from the original rocks; (iv) K_2O was added in Sericite, K-feldspar-sericite and Albite zones, however, depleted in Quartz, Pyrophyllite and Pyrophyllite-sericite zones; (v) Neither large depletion nor large addition of Na_2O occurred in Albite zone, while in K-feldspar-sericite zone, Roseki ore, and Quartz zone Na_2O was depleted to the solution.

(3) Thermochemical consideration, fluid inclusion study, chemical compositions of altered rocks and minerals (sericite, feldspars), and mobility calculation indicate (i) Solution I, which is defined as the hydrothermal solution initially ascending through the column of the original rocks, was strongly acid, 300–350°C in temperature, and oversaturated with SiO_2; (ii) As the solution infiltrated through the column, pH increased from 4.5 in Solution II defined as the solution after the formation of Quartz zone to 6.9 in Solution III defined as the solution after the formation of Roseki ore; (iii) Na remained relatively constant; (4) K and SiO_2 decreased from 0.016 to 0.010 wt.% and from 0.132 to 0.032 wt.% in Solution II and Solution III, respectively.

Further study ought to include statistical approach for the chemical analysis data and more recent reliable thermochemical data to improve our estimation of the chemical compositions of the hydrothermal solution. This would be discussed in a separate paper.

Acknowledgments—We would like to acknowledge Emeritous Prof. J. T. Iiyama of the University of Tokyo for his advise about the consideration of alteration process. The authors also thank to Emeritous Prof. S. Takenouchi of the University of Tokyo who kindly provided laboratory facilities for fluid inclusion studies. Thanks are also due to the chief geologist, Mr. S. Tsushima of the Ohira Mining Co. Ltd. for his help during the field survey.

REFERENCES

Ellis, A. J. (1970) Quantitative interpretation of chemical characteristics of hydrothermal systems. *Geothermics* (Special Issue 2) **2** (Part 1), 516–528.

Ellis, A. J. and Mcfadden, I. M. (1972) Partial molal volume of ions in hydrothermal solutions. *Geochim. Cosmochim. Acta* **36**, 413–426.

Eugster, H. P., Albee, A. L., Bence, A. E., Thompson, J. B., Jr. and Waldbaum, D. R. (1972) The two-phase region and exess mixing properties of paragonite-muscovite crystalline solution. *J. Petrol.* **13**, 147–179.

Fujii, N., Kamitani, M. and Hirano, H. (1971) Study on the Roseki Deposits in Mitsuishi area, Okayama Prefecture, West Japan (Part 1)—"Roseki" Deposits of the Yagi and Umetani Mines—. *Bull. Geol. Surv. Japan* **22**, 473–486 (in Japanese).

Fujii, N., Hirano, H., Sudo, S., Kamitani, M. and Togashi, Y. (1979) Geologic features related to formation of the pyrophyllite and sericite clay (roseki) deposits in the Mitsuishi area, Southwest Japan. *Mining Geol.* **29**, 83–95.

Helgeson, H. (1969) Thermodynamics of hydrothermal system at elevated temperatures and pressures. *Am. J. Sci*. **267**, 729–804.

Helgeson, H., Delany, J. M., Nesbett, H. W. and Bird, D. K. (1978) Summary and critique of the thermodynamic properties of rock forming minerals. *Am. J. Sci*. **278-A**, 229 pp.

Hemley, J. J., Montoya, J. W., Marinenko, J. W. and Luce, R. W. (1980) Equilibria in the system Al_2O_3-SiO_2-H_2O and some general implications for alteration/mineralization process. *Econ. Geol*. **75**, 210–228.

Hirano, H., Fujii, N. and Kamitani, M. (1972) Study on the Roseki deposits in Mitsuishi area, Okayama Prefecture, West Japan (Part 4)—"Roseki" Deposits of the Gotanda Mine—. *Bull. Geol. Surv. Japan* **23**, 275–285 (in Japanese).

Ishihara, S. and Imaoka, T. (1999) A proposal of caldera-related genesis for the Roseki deposits in the Mitsuishi mining area, Southwest Japan. *Resource Geol*. **49**, 157–162.

Kamitani, M. and Fujii, N. (1972) Study on the Roseki Deposits in Mitsuishi Area, Okayama Prefecture, West Japan (Part 3)—"Roseki" Deposits of The Tsuchihashi Mine—. *Bull. Geol. Surv. Japan* **23**, 71–84 (in Japanese).

Kimura, M. (1951) On the Mitsuishi Roseki. *J. Geol. Soc. Japan* **57**, 499–508 (in Japanese).

Kitagawa, R., Nishido, H. and Takeno, S. (1988) K-Ar ages of pyrophyllite (Roseki) deposits in the Chugoku district, southwest Japan. *Mining Geol*. **38**, 357–366.

Kitagawa, R., Nishido, H., Hwang, J.-Y. and Yang, P. (1999) Geochronological study of pyrophyllite deposits in east Asia. *Resource Geol. Spec. Issue* **20**, 123–128.

Matsumoto, R. and Urabe, T. (1980) An automatic analysis of major elements in silicate rocks with X-ray fluorescence spectrometer using fused disk samples. *J. Japan Assoc. Mineral. Petrol. Econ. Geol*. **75**, 272–278 (in Japanese).

Mitsuno, C. and Omori, N. (1984) On the rhyolites of the Mitsuishi–Yoshinaga area. In Explanatory Text of the Geological Map of the Mitsuishi–Yoshinaga Area, Okayama Prefecture. *Hiroshima Bureau Intern. Trade Industry*, 1–6 (in Japanese).

Omori, N. (1965) On the features of the Roseki Deposits in Daiyama, Anizaka and their vicinities, Mitsuishi-cho, Okayama Prefecture. *Earth Sci. Rept. Hiroshima Univ*. **14**, 215–232 (in Japanese).

Omori, N. (1966) Relation between the geological structure and Roseki deposits in the southeast parts of Okayama Prefecture. *Earth Sci. Rept. Okayama Univ*. **1**, 11–30 (in Japanese).

Orville, P. M. (1963) Alkali ion exchange between vapor and feldspar phases. *Am. J. Sci*. **261**, 201–237.

Robie, R. A. and Waldbaum, D. R. (1968) Thermodynamic properties of minerals and related substances at 298.15°K and one atmosphere pressure and at high temperatures. *U.S. Geol. Surv. Bull*. **1259**, 256 pp.

Roedder, E. (1979) Fluid inclusions as samples of ore fluids. *Geochemistry of Hydrothermal Ore Deposits* (Barnes, H. L., ed.), 2nd ed. 632–683.

Shibata, K. and Fujii, M. (1971) Study on the Roseki Deposits in Mitsuishi Area, Okayama Prefecture (Part 2)—K-Ar age of sericite ore from the Yagi Mine—. *Bull. Geol. Surv. Japan* **22**, 575–579 (in Japanese).

Thompson, J. B., Jr. and Waldbaum, D. R. (1968) Mixing properties of sanidine crystalline solutions. 1. Calculation based on ion exchange data. *Am. Mineral*. **53**, 1965–1999.

Yoder, H. S. and Eugster, H. P. (1955) Synthetic and natural muscovite. *Geochim. Cosmochim. Acta* **8**, 225–280.

APPENDIX

Chemical compositions of the altered rocks analyzed by XRF. The data 29 and 30, which are from altered tuffaceous shales, are excluded from the calculation of the average compositions of each alteration zone (see pp. 268–269).

Alteration zone	Weakly propylitized zone					Albite zone					
Data No.	1	2	3	4	Average	5	6	7	8	9	10
Sample No.	71711	40311	40310	40501		41212	41301	42001	110511	110907	110405
SiO_2	68.32	68.88	65.68	68.02	67.72	79.65	73.25	79.70	73.83	70.75	76.62
TiO_2	0.47	0.47	0.46	0.48	0.47	0.14	0.19	0.15	0.17	0.19	0.12
Al_2O_3	15.55	15.62	16.78	15.96	15.98	14.14	14.27	13.83	13.23	13.79	12.49
Fe_2O_3	4.02	3.22	5.34	3.63	4.05	2.46	2.79	1.42	2.33	2.97	2.03
MnO	0.05	0.07	0.07	0.06	0.06	0.04	0.05	0.04	0.05	0.05	0.04
MgO	0.58	0.63	1.30	0.85	0.84	0.28	0.21	0.14	0.28	0.35	0.56
CaO	2.86	3.78	2.85	3.54	3.26	0.85	0.85	1.36	1.88	2.59	1.36
Na_2O	2.81	2.83	2.85	3.52	3.00	2.60	3.73	3.17	2.56	1.81	1.64
K_2O	3.13	2.65	2.13	2.49	2.60	3.32	3.66	3.51	3.62	3.16	4.23
P_2O_5	0.20	0.21	0.13	0.14	0.17	0.08	0.08	0.09	0.13	0.14	0.09
$H_2O(-)$	0.37	0.37	0.33	0.11	0.30	0.19	0.07	0.21	0.10	0.22	0.13
Ignition loss	1.73	0.98	2.71	1.30	1.68	1.68	0.89	1.00	2.35	2.24	2.35
Total (Wt%)	100.09	99.71	100.61	100.11	100.13	105.43	100.04	104.62	100.51	98.25	101.65
Rb (ppm)	150	157			154				258	206	213
Sr (ppm)	281	305			293				186	261	120

Alteration zone	Albite zone								K-feldspar-Sericite zone		
Data No.	11	12	13	14	15	16	17	Average	18	19	20
Sample No.	41723	41601	41819	110509	41317	111401	41125		110412	110415	110402
SiO_2	77.84	78.36	76.05	76.62	80.12	73.63	74.58	76.23	77.68	76.60	82.57
TiO_2	0.07	0.09	0.25	0.16	0.13	0.19	0.23	0.16	0.09	0.07	0.13
Al_2O_3	13.01	12.38	15.07	13.20	13.09	15.93	14.60	13.77	12.95	13.17	12.69
Fe_2O_3	0.33	0.87	2.89	2.16	1.67	2.35	2.01	2.02	1.24	0.93	1.64
MnO	0.00	0.00	0.05	0.04	0.03	0.03	0.03	0.04	0.00	0.03	0.00
MgO	0.04	0.09	0.52	0.15	0.24	0.13	0.13	0.24	0.07	0.25	0.07
CaO	0.08	0.44	2.01	0.46	0.27	1.00	0.80	1.07	0.04	0.02	0.04
Na_2O	3.29	3.35	3.31	1.83	2.72	2.70	3.42	2.78	0.36	0.23	0.67
K_2O	3.84	4.61	3.49	3.77	4.27	3.93	3.80	3.78	5.29	4.77	4.11
P_2O_5	0.11	0.08	0.10	0.08	0.08	0.07	0.09	0.09	0.13	0.08	0.12
$H_2O(-)$	0.50	0.04	0.07	0.28	0.22	0.26	0.27	0.20	0.35	0.34	0.30
Ignition loss	1.03	0.54	1.53	1.84	1.34	2.09	3.75	1.74	1.88	2.60	2.09
Total (Wt%)	100.16	100.84	105.33	100.58	104.17	102.30	103.71	102.12	100.07	99.09	104.43
Rb (ppm)	259							234	226	272	224
Sr (ppm)	91							165	58	63	26

Alteration zone	K-feldspar-Sericite zone				Sericite zone						
Data No.	21	22	23	Average	24	25	26	27	28	29	Average
Sample No.	70606	110408	111613		71113	71514	71501	71011	72001	71502	
SiO_2	79.60	85.10	80.48	80.34	81.93	77.28	78.10	87.23	79.51	80.03	80.81
TiO_2	0.18	0.10	0.06	0.11	0.15	0.08	0.14	0.09	0.11	0.13	0.11
Al_2O_3	11.48	11.99	11.97	12.38	11.09	15.70	15.72	10.24	13.34	12.22	13.22
Fe_2O_3	1.81	0.98	0.22	1.14	0.25	0.09	0.46	0.00	0.84	1.25	0.33
MnO	0.00	0.00	0.00	0.01	0.00	0.00	0.00	0.00	0.01	0.00	0.00
MgO	0.10	0.20	0.21	0.15	0.02	0.05	0.27	0.01	0.16	0.13	0.10
CaO	0.04	0.04	0.18	0.06	0.02	0.02	0.09	0.10	0.11	0.06	0.07
Na_2O	0.17	0.17	0.54	0.36	0.19	0.66	0.83	0.62	0.63	0.54	0.59
K_2O	4.86	5.75	7.65	5.41	2.37	4.60	3.83	2.24	3.43	2.84	3.29
P_2O_5	0.15	0.15	0.14	0.13	0.05	0.05	0.12	0.07	0.08	0.14	0.07
$H_2O(-)$	0.23	0.12	0.20	0.26	0.26	0.22	0.33	0.15	0.19	0.28	0.23
Ignition loss	2.51	1.61	0.79	1.91	1.80	2.57	2.44	1.88	2.06	2.54	2.15
Total (Wt%)	101.12	106.21	102.44	102.23	98.12	101.30	102.33	102.64	100.48	100.15	100.97
Rb (ppm)				241	162	185	224			202	190
Sr (ppm)				49	40	20	40			34	33

Alteration zone	Pyrophyllite-sericite zone				Pyrophyllite zone					Quartz zone		
Data No.	30	31	32	Average	33	34	35	36	Average	37	38	Average
Sample No.	71402	71114	110802		111605	70321	70315	70317		70409	71307	
SiO_2	68.51	76.03	83.86	79.94	81.47	80.04	75.95	67.80	76.32	97.77	97.13	97.45
TiO_2	0.31	0.25	0.11	0.18	0.29	0.15	0.21	0.30	0.24	0.12	0.06	0.09
Al_2O_3	25.20	14.55	12.26	13.40	15.59	15.34	19.14	23.27	18.34	0.42	0.58	0.50
Fe_2O_3	0.18	2.92	0.01	1.46	0.00	1.20	0.03	0.00	0.31	0.00	0.38	0.19
MnO	0.00	0.00	0.00	0.00	0.00	0.00	0.00	0.00	0.00	0.00	0.00	0.00
MgO	0.04	0.05	0.06	0.05	0.03	0.07	0.00	0.03	0.03	0.10	0.04	0.07
CaO	0.03	0.04	0.04	0.04	0.04	0.11	0.09	0.11	0.09	0.02	0.01	0.01
Na_2O	0.44	0.33	0.29	0.31	0.28	0.64	0.72	0.73	0.59	0.25	0.21	0.23
K_2O	0.70	2.94	1.19	2.06	0.03	0.08	0.06	0.09	0.07	0.07	0.09	0.08
P_2O_5	0.18	0.13	0.13	0.13	0.20	0.08	0.09	0.09	0.11	0.07	0.08	0.08
$H_2O(-)$	0.48	0.38	0.50	0.44	0.03	0.25	0.20	0.11	0.15	0.00	0.26	0.13
Ignition loss	4.92	2.01	1.03	1.52	2.94	3.47	4.21	4.90	3.88	0.75	0.86	0.81
Total (Wt%)	100.98	99.62	99.48	99.55	100.90	101.43	100.70	97.43	100.12	99.56	99.70	99.63
Rb (ppm)	120	216	108	162						152	160	156
Sr (ppm)	240	63	25	44						30	48	39